MHCII glycosylation modulates *Bacteroides fragilis* carbohydrate antigen presentation

Sean O. Ryan, Jason A. Bonomo, Fan Zhao, and Brian A. Cobb

Department of Pathology, Case Western Reserve University School of Medicine, Cleveland, OH 44106

N-linked glycans are thought to protect class II major histocompatibility complex (MHC) molecules (MHCII) from proteolytic cleavage and assist in arranging proteins within the immune synapse, but were not thought to directly participate in antigen presentation. Here, we report that antigen-presenting cells (APCs) lacking native complex N-glycans showed reduced MHCII binding and presentation of the T cell activating glycoantigen (GlyAg) polysaccharide A from *Bacteroides fragilis* but not conventional peptides. APCs lacking native N-glycans also failed to mediate GlyAg-driven T cell activation but activated T cells normally with protein antigen. Mice treated with the mannosidase inhibitor kifunensine to prevent the formation of complex N-glycans were unable to expand GlyAg-specific T cells in vivo upon immunization, yet adoptive transfer of normally glycosylated APCs into these animals overcame this defect. Our findings reveal that MHCII N-glycosylation directly impacts binding and presentation of at least one class of T cell–dependent antigen.

CORRESPONDENCE
Brian A. Cobb:
brian.cobb@case.edu

Abbreviations used: βME, β-mercaptoethanol; BMDC, BM-derived DC; CS, castanospermine; GlyAg, glycoantigen; GM-CSF, granulocyte-macrophage colony-stimulating factor; IBD, inflammatory bowel disease; KF, kifunensine; MBPp, myelin basic protein peptide; PHA-L, *Phaseolus vulgaris* leucoagglutinin; PSA, polysaccharide A; TLR, Toll-like receptor; UNT, untreated.

Nearly all mammalian immune system molecules found on the cell surface are glycosylated, including Toll-like receptors (TLRs), class I and II MHC proteins (MHCI and MHCII), CD1, and αβ TCRs. Complex asparagine (N)-linked glycans can reach 30 Å in length (Rudd et al., 1999), which is comparable to the size of a protein Ig domain, and many of these surface glycoproteins have multiple sites of glycosylation. For molecules of the adaptive immune response (e.g., MHCII and TCRs), these glycans are thought to play three primary roles: a check point for proper protein folding and trafficking to the cell surface (Bergeron et al., 1998; Trombetta and Helenius, 1998; Saito et al., 1999), protection of the protein backbone from proteolysis once on the cell surface to maximize the lifetime of cell communication events (e.g., T cell activation; Wormald and Dwek, 1999), and promotion of the appropriate geometric spacing of receptors and other molecules on the cell surface for optimized cell–cell attachment and communication (e.g., the immune synapse; Dustin et al., 1997).

A central player in the adaptive immune response is MHCII, which presents exogenous peptide antigens to TCRs on $CD4^+$ T cells for recognition and T cell activation. The MHCII allele families carry two glycosylated asparagine residues that are highly conserved across species. For the human MHCII molecule HLA-DR2 (DRA, DRB1*1501), there are three known glycosylated sites: N78, N118, and N103 (Fig. 1 A; Gauthier et al., 1998). Published findings demonstrate that these glycans do not play a direct role in antigen binding or presentation, which is elegantly illustrated by crystal structures of nonglycosylated MHCII–peptide complexes expressed in bacteria (Frayser et al., 1999; Li et al., 2000, 2001).

Recently, a new class of T cell–dependent antigens has been described that includes capsular polysaccharides from types 5 and 8 *Staphylococcus aureus* (Tzianabos et al., 2001), type I *Streptococcus pneumoniae* (Sp1; Tzianabos et al., 1993; Stingele et al., 2004; Matsuda and Cepko., 2007; Velez et al., 2009), pneumococcal C-substance (Tzianabos et al., 1993), and polysaccharide A (PSA) and polysaccharide B (Tzianabos et al., 1992, 1993, 1995) from the gut commensal bacteria *Bacteroides fragilis*. Both Sp1 and PSA associate with MHCII molecules in professional APCs and are recognized by TCRs on $CD4^+$ T cells (Tzianabos et al., 1993; Cobb et al., 2004; Cobb and Kasper, 2008; Velez et al., 2009). Sp1 and PSA both form highly charged right-handed helices with two repeating units per

The Rockefeller University Press $30.00
J. Exp. Med. Vol. 208 No. 5 1041-1053
www.jem.org/cgi/doi/10.1084/jem.20100508

turn and a pitch of 20 Å (Wang et al., 2000; Choi et al., 2002), whereas initial recognition of these "glycoantigens" (GlyAg) leads to cytokine production (e.g., IFN-γ) and T cell proliferation (Brubaker et al., 1999; Stingele et al., 2004; Stephen et al., 2005) with an overall phenotype indistinguishable from T helper type I (T_H1) cells. GlyAg association with HLA-DR2 (DR2) shows high affinity (K_d = 315 nM; Cobb and Kasper, 2008), is dependent on positive and negative charges found within the polysaccharide (Kreisman et al., 2007; Cobb and Kasper, 2008; Velez et al., 2009), and requires processing via nitric oxide to fragments in the 5–10 kD size range (Cobb et al., 2004; Velez et al., 2009). Although GlyAg–MHCII binding is competitive with peptide antigens and requires the expression of HLA-DM in APCs for presentation (Cobb and Kasper, 2008; Velez et al., 2009), the manner in which GlyAgs interact with MHCII remains unknown.

Here, we present a study in which it was discovered that bacterially expressed DR2 failed to associate with GlyAg despite being properly folded and fully capable of binding to antigenic peptide. We also show that elimination of native complex N-linked glycans (i.e., unaltered mammalian complex N-glycans) on MHCII reduced presentation of GlyAg in live APCs, nearly eliminates GlyAg binding to recombinant MHCII in vitro, and significantly limits in vitro and in vivo GlyAg-mediated T cell recognition and activation despite no detectable defects in peptide and intact protein antigen controls. In contrast to the current model, our findings reveal that the nature of the N-glycans found on MHCII can directly modulate antigen binding and presentation. Because T cell recognition of GlyAg is critical for gut immune homeostasis (Mazmanian et al., 2005, 2008), these results raise intriguing questions about the variability of MHCII glycosylation in the gut (Barrera et al., 2002) and how inflammation-associated variability could modulate antigen presentation and T cell responses against the commensal microbiota.

RESULTS

Native MHCII N-glycans are required for GlyAg presentation

Although MHCII glycosylation does not appear to play a direct role in conventional peptide antigen binding (Frayser et al., 1999; Li et al., 2000), we sought to determine the functional role of these glycan structures during commensal-derived GlyAg presentation. Human Raji B cells, which have been previously demonstrated to present GlyAg via MHCII binding (Cobb et al., 2004), were cultured in the presence and absence of the glucosidase inhibitor castanospermine (CS; 175 μM) or the mannosidase inhibitor kifunensine (KF; 10 μg/ml) for 3 d to reduce the presence of hybrid and native complex

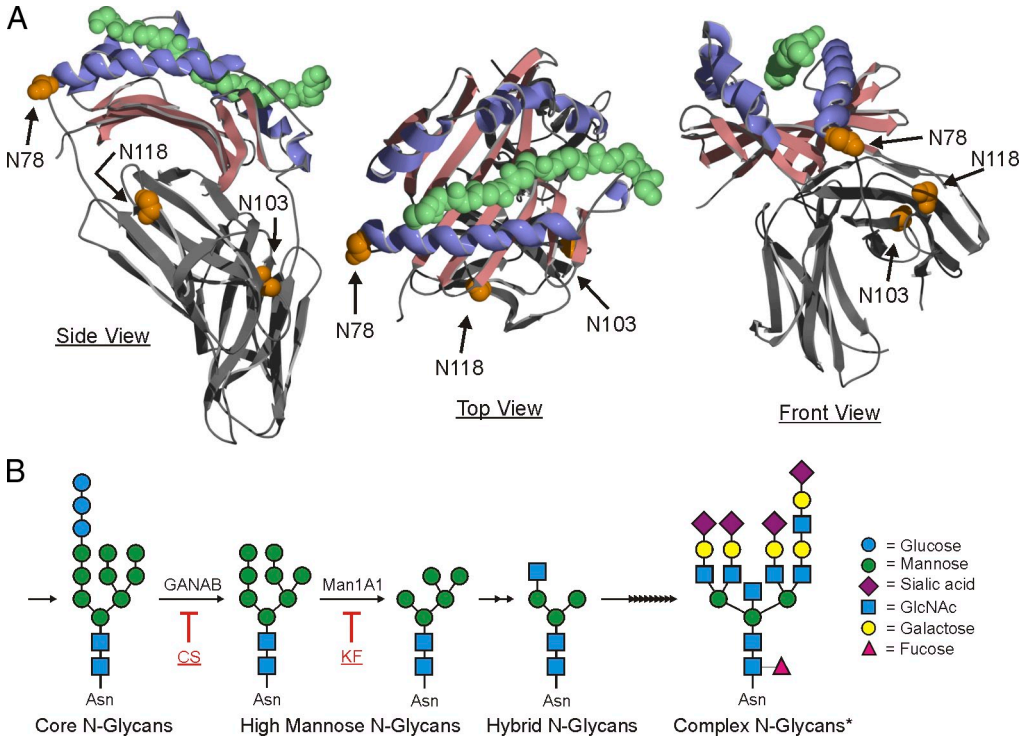

Figure 1. HLA-DR2 glycosylation sites and mechanism. (A) HLA-DR2 (DRA; DRB1*1501), shown with myelin basic protein peptide (green; space-filling), contains three N-glycosylation sites. The N78 position is highly conserved across species and is located at one end of the canonical peptide-binding groove, which is comprised of α-helices (blue) and a β-sheet foundation (red). Coordinates are from Gauthier et al., 1998. (B) Simplified N-glycosylation pathway in mammalian cells, highlighting the sites of CS (glucosidase inhibitor) and KF (mannosidase inhibitor) action and the representative structures expected. The asterisk highlights a complex N-glycan example from public data via the Consortium for Functional Glycomics. Specifically, this structure was found expressed by murine RAW macrophages, has a mass of 5035.3 Daltons, and is available in the dataset for A. Merrill request #1689 (http://www.functionalglycomics.org/glycomics/publicdata/glycoprofiling-new.jsp).

N-glycans on cellular glycoproteins (Fig. 1 B). On the fourth day, the cells were provided fresh drug and either biotinylated myelin basic protein peptide (MBPp) or biotinylated glycoantigen PSA from *B. fragilis* and allowed to incubate for another 24 h. The MHCII-antigen complexes were subsequently immunoprecipitated with mAb against MHCII (clone L243) and probed with streptavidin to quantify the presented antigen. We found no difference in the amount of MBPp presented by the cells treated with either inhibitor (Fig. 2, A and B) when compared with untreated cells (UNT), yet cells treated with CS or KF showed significant reductions in the amount of GlyAg presented (Fig. 2, A and B).

Given that CS and KF affect all N-glycosylated proteins in the cell, we used identically treated Raji B cells in flow cytometry experiments to measure surface-localized MHCII molecules. No difference was detected in the surface concentration of MHCII (Fig. 2, C and D). We also used FITC-conjugated lectins to stain the cells and found the expected reductions in *Phaseolus vulgaris* leucoagglutinin (PHA-L), PHA-E, and WGA lectin staining with concomitant increases in Con A staining in CS- and KF-treated populations (Fig. 2, C and D), suggesting that the glycans present had increased mannose compositions. To ensure that CS and KF did not affect cell viability, the metabolic state of the cells were assessed by measuring ATP production (Fig. 2 E). No reduction in cellular metabolic activity (i.e., ATP production) was seen between UNT and inhibitor-treated cells. Finally, it has been previously reported that PSA and other GlyAgs require intracellular processing via a nitric oxide–dependent pathway. To ensure that the treated Raji B cells processed PSA normally, full-length radiolabeled PSA was given to the cells, and then isolated from the endosomal compartments after overnight incubation. The endosomal PSA was then passed through an analytical molecular sieve column to measure the molecular size. We found that all cells equally endocytosed and processed PSA into two molecular mass populations (Fig. 2 F, arrows) as previously published (Cobb et al., 2004).

CS- and KF-treated Raji B cells were also compared with UNT cells by confocal microscopy. The cells were given inhibitor for 3 d before incubation with either AlexaFluor594-conjugated PSA (red) or DQ-OVA (shown in red), which is fluorescent only after proteolytic processing into peptides (Lewis and Cobb, 2010). After 24 h of antigen exposure, the cells were fixed with 4% paraformaldehyde, stained with Alexa Fluor 488– or Alexa Fluor 633–conjugated MHCII mAb (shown in green for both), and viewed by confocal microscopy (Fig. 3, A and C). We found no detectable difference in MHCII staining as a function of drug treatment. In addition, the presence of bright DQ-OVA signal at the cell surface indicates that there was no significant difference in OVA processing or surface localization. In contrast, a reduction in surface colocalization of PSA in cells treated with CS or KF (lack of yellow colocalization signal in overlay images) was observed. Using a series of images ($n = 8$), we analyzed the pixel intensity distribution within each cell for each antigen. We found highly significant reductions ($P < 0.01$) in

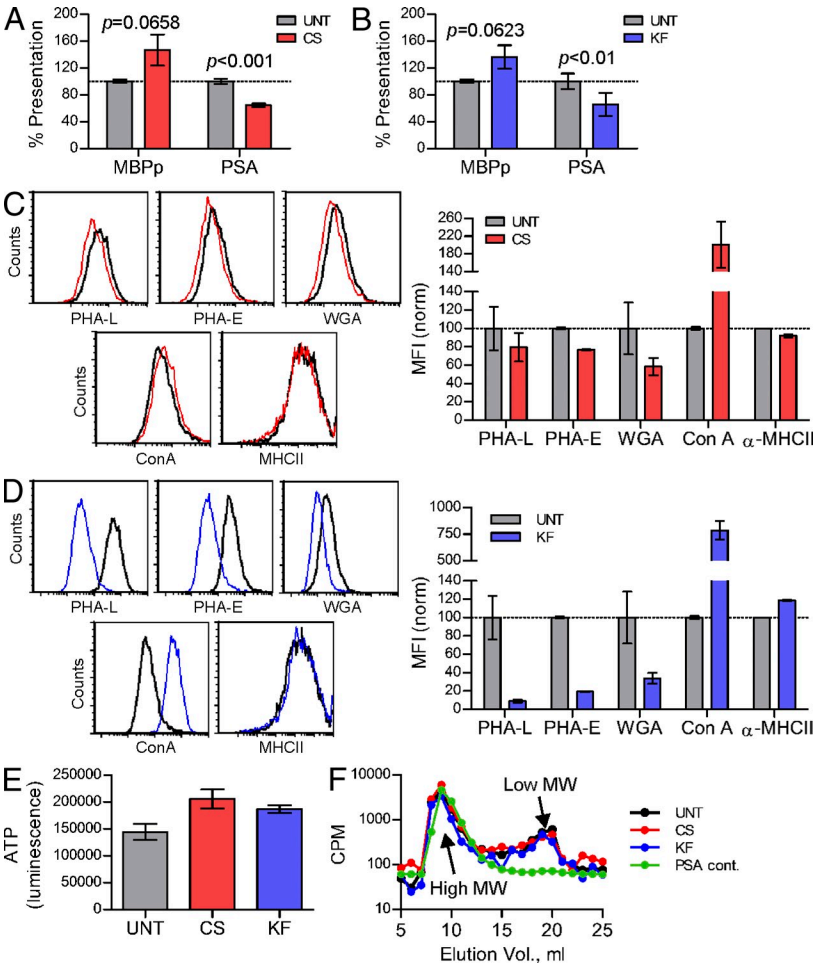

Figure 2. B cells lacking native N-glycans show reduced PSA presentation. (A and B) Coimmunoprecipitations (coIP) with α-MHCII mAb from CS- and KF-treated Raji B cells show reduced PSA (CS, $P < 0.001$; KF, $P < 0.01$), but not MBP peptide ($P > 0.05$), presentation compared with untreated (UNT) controls. $n = 12$ for all PSA; $n = 15$ for all MBPp. (C and D) Flow cytometry of UNT, CS-treated (C), and KF-treated (D) Raji B cells using lectin staining to detect the glycophenotype of the cell surface. Representative histograms are shown; $n = 4$ for each data point. (E) ATP production of UNT, CS-treated, and KF-treated Raji B cells. $n = 3$ for each data point. (F) [^{3}H]-labeled PSA isolated from endosomal compartments was analyzed from UNT, CS-treated, and KF-treated Raji B cells and compared with intact, full-length PSA control (PSA cont.) by size exclusion HPLC using a Superose 12 column. The arrow indicates low molecular mass PSA. Representative elution profiles are shown. All bar graphs show the mean ± SEM.

surface-localized PSA (Fig. 3 B), but not DQ-OVA (Fig. 3 D) signal in CS- and KF-treated cells compared with UNT, but little difference seen within the cells (Fig. 3, B and D).

The results shown in Figs. 2 and 3 collectively demonstrate that modification of N-glycans on MHCII proteins in human B cells reduces MHCII-dependent presentation of GlyAg, but not conventional peptide or intact protein antigens, and that this alteration is not caused by changes in cell viability, MHCII expression or trafficking, or GlyAg processing.

CS and KF reduce native complex N-glycans in Chinese hamster ovary (CHO) cells expressing recombinant HLA-DR2

Defects in GlyAg presentation within the context of live APCs could result from several processes that may be altered with CS and KF treatment, such as defects in HLA-DM activity or cathepsin activity to cleave the invariant chain (Ii) from the MHCII complex. To determine whether the observed defect was caused by deficiencies in GlyAg binding to MHCII, recombinant HLA-DR2 (DR2) was expressed in CHO cells in the presence and absence of CS and KF. The UNT, CS, and KF grown DR2 molecules (UNT-DR2, CS-DR2, and KF-DR2) were purified to homogeneity using an L243 mAb affinity column as previously described (Cobb et al., 2004).

To confirm the effectiveness of CS and KF, the CHO cells were analyzed by fluorescent lectin staining and flow cytometry. In both cases, CS and KF significantly reduced PHA-L binding to the cell surface, demonstrating the elimination of native complex N-glycans on all proteins expressed by the cells (Fig. 4, A and B). To better characterize the N-glycans present on the purified DR2 samples, a panel of lectins was used in ELISA assays. CS-DR2, KF-DR2, and UNT-DR2 were captured in wells precoated with L243 mAb and then probed with FITC-conjugated lectins to quantify the types of glycans present in the DR2 samples (Fig. 4, C and D). We found no change in succinylated WGA (S-WGA) binding and increased Con A binding, but reductions in PHA-L, WGA, GSL I, STL, and UAE I lectin binding for CS-DR2 and KF-DR2 compared with UNT-DR2. These data indicate significant modification of native N-glycans (PHA-L), fucosylation (UAE I), α-linked galactose residues (GSL I), and terminal sialic acids (WGA and STL). The retention of S-WGA binding suggests that GlcNAc residues, which are found in the early core glycan structures (Fig. 1 B), remain. Likewise, the increased Con A staining demonstrates retention of mannose and/or glucose residues, typical of early core structures, within the glycans. Overall, the lectin screen demonstrates that the recombinant CS-DR2 and KF-DR2 lack the native complex N-glycans found in UNT-DR2.

MHCII binding to GlyAg requires both the protein backbone and native complex N-glycans

Bacteria-expressed nonglycosylated DR2 (Bac-DR2) and CHO-expressed UNT-DR2 were used in quantitative binding assays with 10 µg/ml biotinylated MBPp or biotinylated low

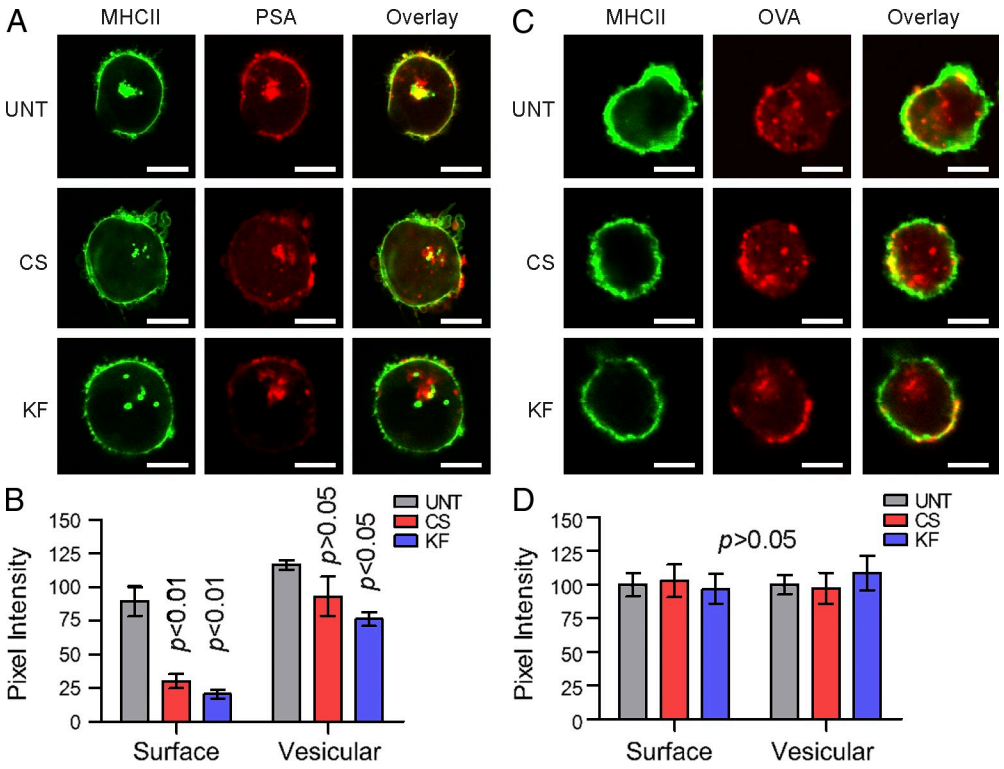

Figure 3. B cells lacking native N-glycans show internal but not surface MHCII–PSA colocalization. (A and B) Uptake of PSA (red) in UNT, CS-treated, and KF-treated Raji B cells. Intracellular colocalization with MHCII protein (green) is shown in yellow. (C and D) DQ-OVA was used as an intact protein antigen control, which fluoresces only after proteolytic cleavage (Lewis and Cobb, 2010). Representative images are shown; Bars, 10 µm. $n = 8$ for quantification. All bar graphs show the mean ± SEM.

molecular weight PSA as previously described (Cobb et al., 2004; Cobb and Kasper, 2008). We found that PSA binding to Bac-DR2 was significantly reduced compared with the fully glycosylated UNT-DR2, whereas the binding of MBPp increased with the Bac-DR2 (Fig. 4 E). We also compared UNT-DR2 with CS-DR2 and KF-DR2 and found no change in conventional peptide antigen binding, but a 75% reduction in GlyAg binding (Fig. 4, F and G). Because PSA is a highly charged antigen that is known to depend upon charges for MHCII binding (Kreisman et al., 2007; Cobb and Kasper, 2008), we treated UNT-DR2 with neuraminidase to remove negatively charged terminal sialic acids. Lectin ELISA confirmed the reduction of sialic acids (Fig. 4 H) and the neuraminidase-digested protein antigen binding was compared with the binding to native UNT-DR2 (Fig. 4 I). We found a small, but statistically insignificant, change in overall binding of both GlyAg and conventional peptide, demonstrating that the negative charges provided by terminal sialic

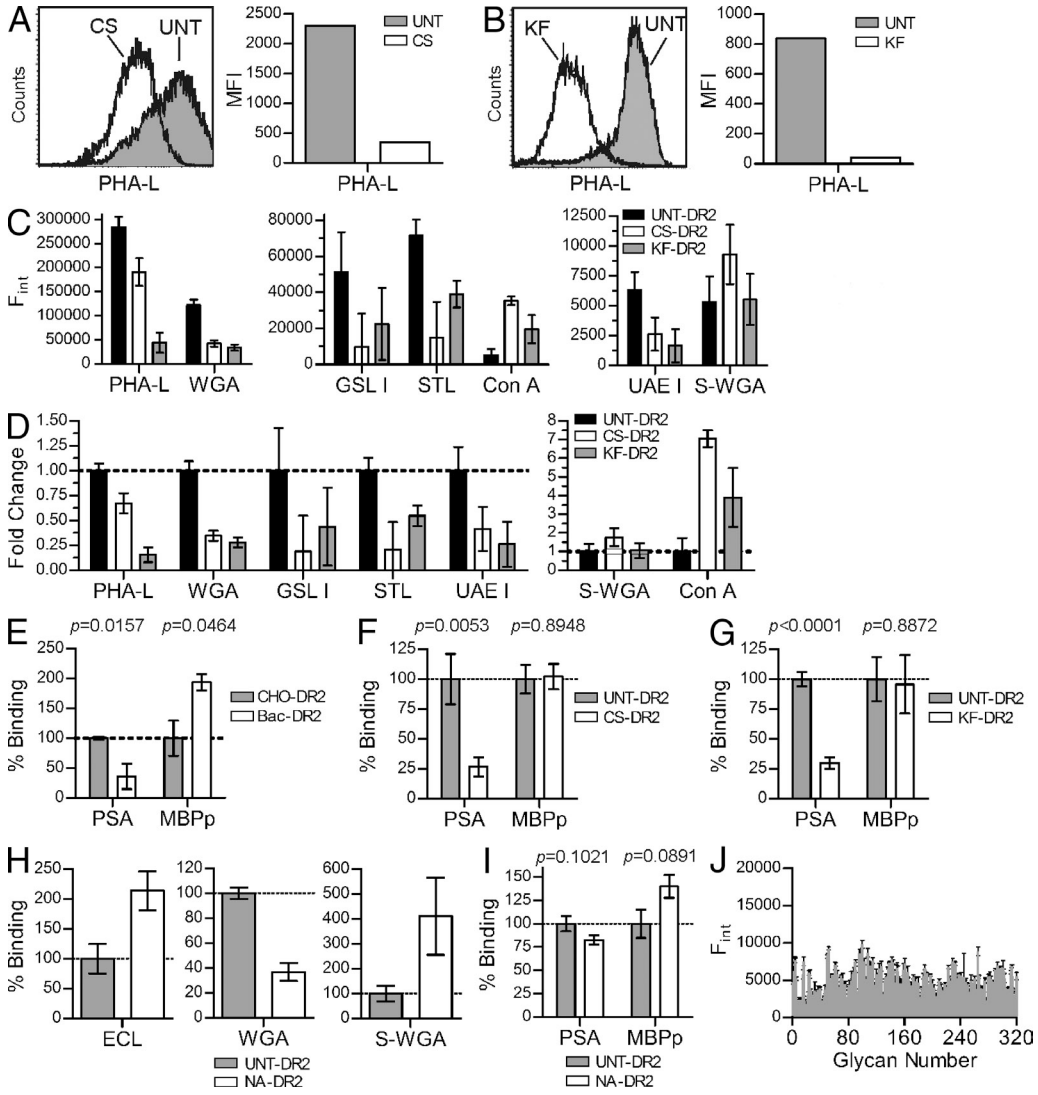

Figure 4. Both native N-glycans and the HLA-DR2 protein backbone are required for PSA binding. (A and B) Flow cytometry analysis of CS- and KF-treated CHO cells were compared with UNT cells using a lectin sensitive to the presence of native complex N-glycans. Representative histograms are shown. (C and D) HLA-DR2 expressed by UNT, CS-treated, and KF-treated CHO cells was immobilized and probed using a panel of FITC-conjugated lectins to detect changes in MHCII glycosylation. The raw data showing relative concentrations of the target glycan structure (D) and fold change (E) of each lectin is shown. $n = 9$ per data point. (E) Quantitative binding experiments using PSA or MBPp with purified HLA-DR2 expressed in bacteria (Bac-DR2; nonglycosylated) or DR2 expressed in CHO cells (CHO-DR2; fully glycosylated). $n = 4$ per data point. (F and G) MBPp and PSA binding to DR2 lacking native N-glycans expressed in CHO cells grown in CS-supplemented ($n = 9$; F) or KF-supplemented media ($n = 18$; G) compared with CHO-DR2 expressed in the absence of inhibitor. (H) Lectin ELISA of neuraminidase-digested CHO-DR2. (I) Native CHO-DR2 enzymatically trimmed with $\alpha(2\rightarrow3,6,8,9)$-neuraminidase (NA-DR2) binding to PSA or MBPp compared with untreated CHO-DR2. $n = 21$. (J) Alexa Fluor 488–conjugated PSA was used as ligand in a glycan-binding array containing 320 glycans (Table S1) at the Consortium for Functional Glycomics. Positive signal is typically above 20,000 U. $n = 4$ per glycan. All bar graphs show the mean ± SEM.

acid residues are not critical for binding, yet native complex N-glycans are necessary for GlyAg but not conventional peptide antigen binding to MHCII molecules.

The binding results suggest that GlyAg molecules may form carbohydrate–carbohydrate interactions with MHCII N-glycans. To determine whether GlyAg can bind to glycans independently from the MHCII protein backbone, Alexa Fluor 488–conjugated PSA was screened for binding against a library of 320 glycans at the Consortium for Functional Glycomics (Fig. 4 J). We found no significant interactions above background with any of the immobilized glycans (see Table S1 for a complete list).

These binding results directly demonstrate that the reduction in MHCII-dependent cell surface presentation of GlyAg is caused by defects in the direct interaction between GlyAg and MHCII. Furthermore, it is clear that neither the MHCII protein backbone nor the N-glycans are independently sufficient for GlyAg binding.

Native complex N-glycans are required for GlyAg-mediated T cell activation in vitro

BM-derived DCs (BMDCs) were cultured for 3 d with and without CS or KF, as performed with the Raji and CHO cells. Fluorescent lectin staining analyzed by flow cytometry verified the loss of native complex N-glycans on CS- and KF-treated cells (Fig. 5 A) and the cells were confirmed as $CD11c^+$ by flow cytometry (Fig. 5 B). On day 4, the cells were provided fresh drug and pulsed with 50 µg/ml PSA or 50 µg/ml OVA peptide (OVAp; residues 323–339) and 20 ng/ml LPS, 20 ng/ml LPS alone, 50 µg/ml DQ-OVA, 50 µg/ml Sp1, 50 µg/ml *B. fragilis* capsule containing polysaccharide B, or no antigen for 24 h. DQ-OVA is intact OVA that is nonfluorescent until cleaved to peptide, thus aliquots of the DQ-OVA–pulsed cells were analyzed by flow cytometry to verify protein uptake and processing. No difference was seen between UNT, CS-, and KF-treated BMDCs (Fig. 5 C).

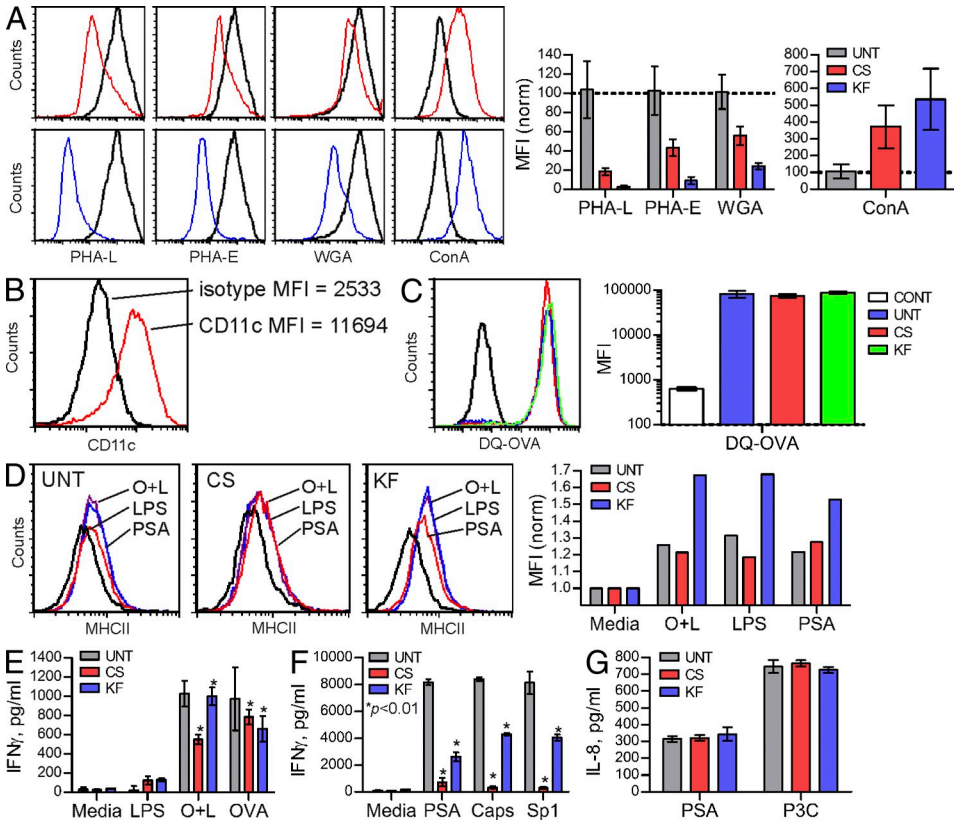

Figure 5. Native complex N-glycans are required for PSA-driven T cell activation in vitro. (A) BMDCs were cultured in the presence or absence of CS (red) and KF (blue) for 3 d, and then analyzed by PHA-L, PHA-E, WGA, and Con A lectin flow cytometry to detect N-glycans. Representative histograms and $n = 4$ MFI analyses are shown. (B) BMDCs were cultured for 8 d, probed with CD11c mAb, and analyzed by flow cytometry to verify proper DC cell differentiation. Representative histogram is shown. (C) BMDCs were incubated with nonfluorescent intact DQ-OVA protein for 24 h to allow uptake and processing. Cells were then analyzed for fluorescence, which is indicative of endocytosis and cleavage to peptides. Representative histograms are shown. $n = 4$ for MFI analyses. (D) BMDC maturation upon exposure to antigen was measured by surface staining of MHCII 24 h after stimulation with OVA peptide and LPS (O+L), LPS alone, or PSA. Representative histograms shown. (E) BMDCs grown with and without CS and KF were pulsed with either DQ-OVA (OVA), OVAp+LPS (O+L), or LPS alone for 24 h, after which untreated fresh naive $CD4^+$ T cells isolated from OT-II animals were added. $n = 3$ per condition, per antigen. (F) As with OVAp, BMDCs were grown with CS and KF and pulsed with PSA, Sp1, or *B. fragilis* capsule (Caps) for 24 h. Next, naive WT C57BL/6 $CD4^+$ T cells were added to allow activation to occur. $n = 3$ per condition. (G) TLR2 activation by PSA, a necessary step in GlyAg-mediated T cell activation (Wang et al., 2006), and a control agonist Pam3Cysk4 (P3C) was measured in untreated (UNT), CS-treated, or KF-treated $TLR2^+$ HEK293 cells. Bars represent background-subtracted values. $n = 3$ per condition. All bar graphs show the mean ± SEM.

A subset of these antigen-pulsed BMDCs were also surface stained with FITC-conjugated MHCII mAb to measure increases in plasma membrane–localized MHCII concomitant with DC maturation (Fig. 5 D). For all antigen combinations, we found equal increases in surface MHCII localization over no antigen controls, thus neither CS nor KF leads to a defect in DC maturation. In fact, KF treatment appears to have increased the MHCII surface concentration above no-inhibitor controls.

The remaining antigen-pulsed BMDCs were cultured with fresh $CD4^+$ T cells from either WT C57BL/6 (PSA, Sp1, and capsule assays) or OT-II (DQ-OVA and OVAp assays) mice to determine the capacity of the BMDCs loaded with antigen to induce T cell activation. At day 3 for DQ-OVA and OVAp assays (Fig. 5 E) or day 4 for the GlyAg assays (Fig. 5 F), culture supernatants were assessed for IFN-γ production by ELISA. We found no significant difference in OT-II T cell activation between treatment groups when stimulated with intact protein antigen DQ-OVA or preprocessed OVAp-pulsed BMDCs, yet all three GlyAg-mediated T cell activation assays were significantly reduced in assays containing BMDCs grown in CS or KF.

Previous findings have reported that GlyAg-mediated T cell activation requires signaling through TLR2 (Wang et al., 2006). To rule out TLR2 as the cause of the lack of T cell activation mediated by GlyAg-pulsed and CS- or KF-grown BMDCs, we cultured $TLR2^+$ HEK293 for 3 d in the presence and absence of CS and KF as before. On day 4, the cells were stimulated for 12 h with either 50 µg/ml PSA or 15 nM Pam-3Cysk4 and culture supernatants assayed for IL-8 by ELISA (Fig. 5 G). We found robust IL-8 production in response to both stimuli and no change in IL-8 production in CS- or KF-treated cells.

Collectively, these data demonstrate that alterations in N-glycan formation in APCs does not affect conventional protein or peptide antigen–mediated T cell activation, but significantly reduces T cell activation by three different GlyAgs.

Native complex N-glycans are required for GlyAg-mediated responses in vivo

Reduction of MHCII binding and presentation of GlyAg negatively effects in vitro T cell recognition and activation. To determine the in vivo effect of the reduction of native complex N-glycans in C57BL/6 mice on GlyAg-mediated responses, animals were injected with 250 µg of KF daily for 1, 2, or 3 d. On day 4, the animals were sacrificed and the bulk splenocytes were assessed by lectin (PHA-L) staining and flow cytometry to test for drug effectiveness (Fig. 6 A). We found that by day 3, essentially all native complex N-glycans were missing from the surface of all splenocytes.

To assess the effect of the 3-d KF treatment regimen on GlyAg-driven immune responses, we challenged the KF and PBS vehicle–treated (UNT) mice with PSA. After 6 d, the spleens were removed and the cells stimulated with PMA/ionomycin

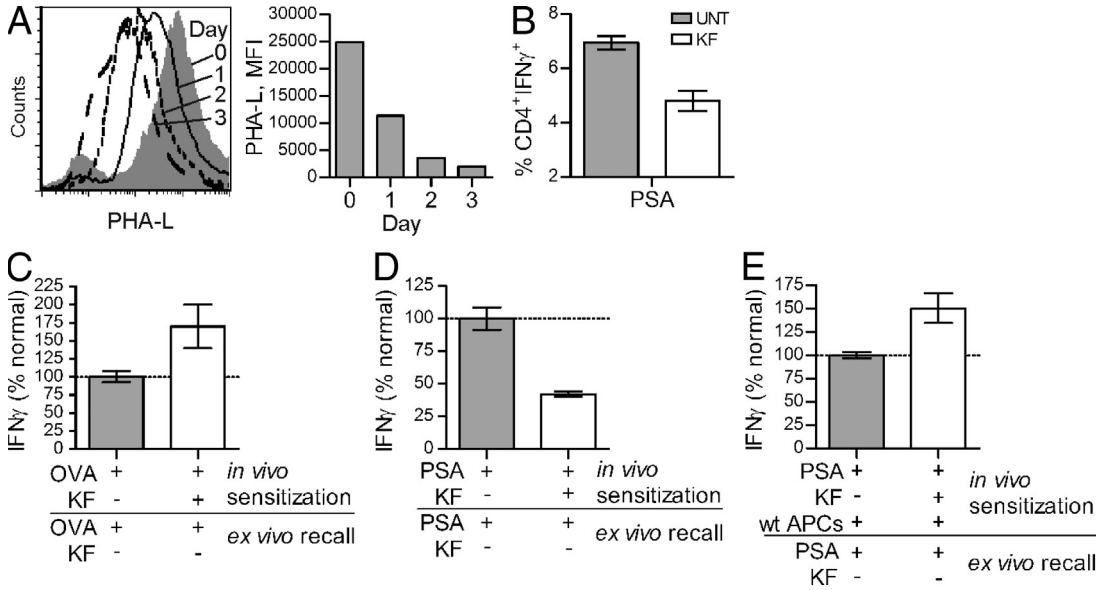

Figure 6. Native complex N-glycans are required for PSA-driven immune responses in vivo. (A) WT C57BL/6 animals ($n = 8$) were treated daily for 1, 2, or 3 d with 250 µg of KF, and then sacrificed to harvest splenocytes. Cells were stained for native complex N-glycans using PHA-L. Representative histogram shown. (B) WT mice ($n = 3$ per group) were treated with KF or PBS for 3 d, as in A. Animals were then sensitized with 100 µg PSA. Splenocytes were harvested 6 d later, stained for IFN-γ and CD4, and analyzed by flow cytometry. (C) KF- or PBS-pretreated mice ($n = 6$) were sensitized with 100 µg OVA and sterile cecal content adjuvant. 4 d later, $CD4^+$ T cells were isolated and restimulated ex vivo with normally glycosylated APCs and OVA ($n = 6$). (D) Animals ($n = 6$) were treated as in C, only with 100 µg of PSA rather than OVA. The PSA-specific recall ($n = 18$) was measured after ex vivo restimulation with normally glycosylated APCs and PSA. (E) Animals ($n = 6$) were treated as in D, only with the additional adoptive transfer of 5×10^6 fresh normally glycosylated APCs at the time of PSA injection ($n = 12$). For panels C–E, data were normalized to the antigen-sensitized animals without KF. All bar graphs show the mean ± SEM.

for intracellular cytokine analysis. We found a significantly higher percentage of $CD4^+$ T cells producing IFN-γ in animals expressing native complex N-glycans compared with animals treated with KF (Fig. 6 B).

To verify that this increase in $CD4^+IFN\gamma^+$ T cell number reflects PSA-specific cells, we performed recall experiments from UNT and KF-treated animals sensitized with PSA or OVA protein. Animals were injected with KF or PBS vehicle for three consecutive days. On the fourth day, the animals were challenged with OVA protein or PSA and allowed to respond for 4–6 d. The $CD4^+$ T cells were then harvested from each animal and restimulated ex vivo with APCs from UNT naive animals (i.e., normally glycosylated cells) and either PSA or OVA to measure the level of immunological recall. We found that with OVA, the number of responding T cells during sensitization in KF-treated animals increased over animals sensitized without KF (Fig. 6 C). In contrast, KF treatment during sensitization with PSA resulted in a decreased T cell response upon recall with PSA compared with UNT animals expressing native complex N-glycans (Fig. 6 D). These data show that KF inhibited PSA-specific T cell expansion during in vivo sensitization. To determine if this inhibition is caused by presentation defects within the resident APCs, KF-treated or UNT animals were sensitized with PSA along with adoptively transferred normally glycosylated APCs isolated from naive mice. Inclusion of normal APCs during PSA sensitization of KF-treated animals allowed for PSA-specific T cell responses in vivo to reach normal levels, as shown by the increased PSA-specific recall response (Fig. 6 E).

MGat2 ablation reduces native complex N-glycans and eliminates GlyAg-mediated T cell activation

Loss of the GlcNAc glycosyltransferase II enzyme (encoded by the *MGat2* gene) in an animal model of the type IIa congenital disorders of glycosylation (CDG-IIa) results in several osteogenic, hematologic, and gastrointestinal tract abnormalities (Wang et al., 2001). The mice lacking *MGat2* also die early in postnatal development and lack native branched complex N-glycans. To determine if genetic-based loss of native complex N-glycans in the APC would also result in GlyAg T cell activation defects, BM was isolated from mice that carry the *MGat2* gene flanked by LoxP sites but do not express the CRE recombinase. BM cells from either WT or $MGat2^{flox}$ animals were either mock electroporated or electroporated with an expression construct for myc-tagged CRE recombinase (pCRE) to excise the floxed *MGat2* gene, and then cultured as usual with granulocyte-macrophage colony-stimulating factor (GM-CSF) to derive dendritic cells. The four resulting populations of BMDCs were analyzed by PHA-L staining to confirm reduction in native complex N-glycans (Fig. 7 A). Approximately 40% of the $MGat2^{flox}$ BMDCs electroporated with pCRE lacked significant PHA-L staining, whereas the mock transfected $MGat2^{flox}$ BMDCs and both WT populations were uniformly PHA-L positive. Unstained controls are shown in Fig. S1 A. NP-40 lysates from these four populations were analyzed using Western blots and probed with either anti-CRE (Fig. 7 B) or anti-myc (Fig. S1 B) antibodies to demonstrate CRE expression. Both WT and $MGat2^{flox}$ cells show CRE expression when electroporated

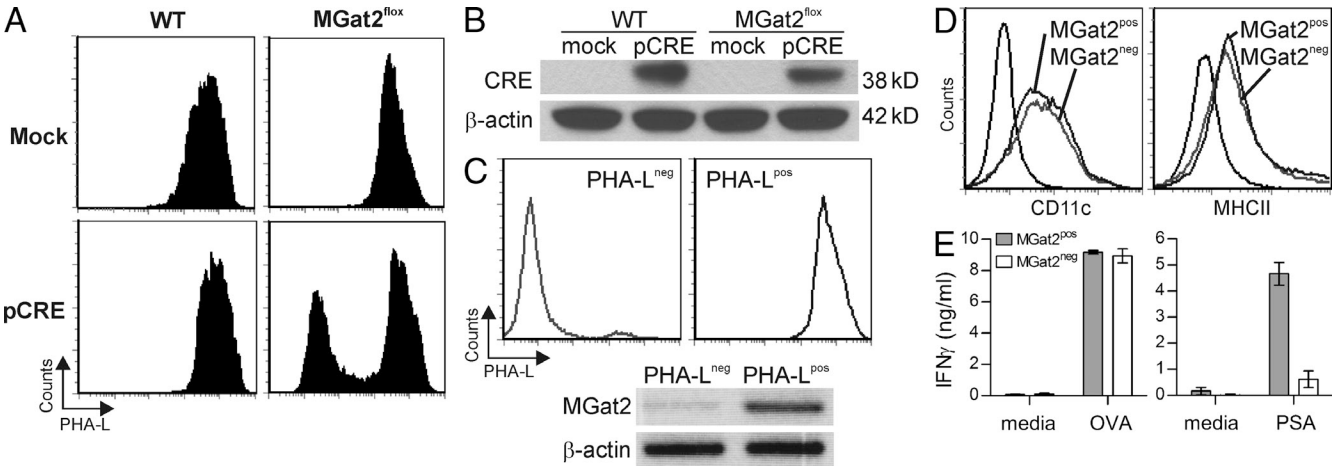

Figure 7. Deletion of *MGat2* results in deficient PSA, but not OVA-mediated T cell activation. (A) BM cells were harvested from $MGat2^{wt}$ (WT) or $MGat2^{flox}$ animals, electroporated with a CRE expression construct (pCRE) or mock electroporated without DNA, and cultured with GM-CSF for DC differentiation. Cells were stained with PHA-L to determine the effect of *MGat2* excision. Representative histograms are shown. (B) Mock and pCRE electroporated BM cells were extracted and lysates were analyzed by anti-CRE Western blot using β-actin as a loading control. Representative blot shown. (C) PHA-L^- pCRE electroporated $MGat2^{flox}$ BMDCs were isolated from PHA-L^+ cells by negative selection using PHA-L and magnetic beads and compared with PHA-L^+ pCRE-electroporated WT cells. Flow cytometry was used to measure the purity and glycophenotype of the populations, whereas RT-PCR on mRNA isolated from the PHA-L^{pos} and PHA-L^{neg} BMDCs was performed to demonstrate the excision of *MGat2* in PHA-L^{neg} BMDCs ($MGat2^{neg}$) but not PHA-L^{pos} BMDCs ($MGat2^{pos}$). Representative histograms and gel shown. (D) Flow cytometry was used to measure BMDC differentiation (CD11c) and MHCII expression (MHCII) in both PHA-L^{pos} and PHA-L^{neg} BMDC populations. Representative histograms shown. (E) $MGat2^{pos}$ and $MGat2^{neg}$ BMDCs were cultured with either OT-II $CD4^+$ T cells and OVA (50 µg/ml) or WT $CD4^+$ T cells and PSA (50 µg/ml). T cell activation was determined by IFN-γ ELISA of the culture supernatants. (n = 3 independent experiments).

with the pCRE but not in mock controls. Using biotinylated PHA-L, the PHA-L$^-$ BMDCs were then isolated by magnetic bead negative selection, reanalyzed for PHA-L staining, and compared with pCRE-electroporated WT BMDCs (Fig. 7 C). The purity of each population was consistently >90% for both PHA-L^{neg} and PHA-L^{pos} BMDCs. mRNA was isolated from the two populations, and the lack of *MGat2* transcript in the PHA-L^{neg} population was confirmed by RT-PCR (Fig. 7 C). As before, the expression levels of CD11c and MHCII were verified and no significant differences were observed (Fig. 7 D). Finally, the MGat2^{pos} and MGat2^{neg} BMDCs were used in T cell activation assays with either OT-II CD4$^+$ T cells (OVA assays) or WT CD4$^+$ T cells (PSA assays). As seen with the CS- and KF-treated BMDCs (Fig. 5), the protein antigen response was unaffected by the loss of MGat2, yet the GlyAg response was nearly eliminated when native complex N-glycans were missing in the BMDCs (Fig. 7 E). These data validate the inhibitor-based observations and confirm that PSA presentation and downstream T cell activation relies upon native complex N-glycosylation of MHCII proteins.

DISCUSSION

Most immune cell surface receptors and accessory molecules are glycoproteins, including CD4, CD8, αβ T cell receptors, and both class I and class II MHC. MHCII-dependent antigen presentation is a central event for adaptive immune responses against extracellular fungi, bacteria, and other pathogens. In this study, modification of MHCII N-glycosylation with N-glycosylation processing enzyme inhibitors (CS or KF) or through CRE-mediated ablation of the *MGat2* gene resulted in the elimination of native complex N-glycans on APCs, which significantly reduced binding, presentation, and T cell activation by the glycoantigen PSA isolated from the capsule of the commensal bacteria *B. fragilis*. The reduction in presentation translated into a reduction in GlyAg-mediated CD4$^+$ T cell activation in vitro and in vivo. These findings demonstrate for the first time that MHCII-mediated binding and presentation of at least one class of antigens depends heavily upon native complex N-glycans decorating the MHCII protein backbone.

Complex N-glycans are large and highly flexible structures that can extend to 30 Å, roughly corresponding to the size of an immunoglobulin domain (Rudd et al., 1999, 2001). These molecules are thought to contribute to the functionality of the underlying protein in several indirect ways. For example, the N-linked glycans attached to the adhesion molecule CD2 near the plasma membrane are thought to structurally restrict the protein conformation such that trans-interactions between CD2 and its ligand CD48 on opposing cells are promoted over cis-interactions between CD2 and CD48 expressed on the same cell (Dustin et al., 1996). This general principle is thought to apply to many of these surface glycoproteins including MHC and TCRs, whereby the glycans can prevent lateral nonspecific aggregation and provide a regular structural lattice for glycoprotein packing on the cell surface (Rudd et al., 1999, 2001). Ordering of surface receptors and adhesion molecules is even thought to contribute to the stability and avidity of the immune synapse formed between APCs and T cells, however, the fundamental binding properties of MHC for peptides and TCRs for the MHC-peptide complex are essentially unaffected by the presence or absence of complex N-glycans. In our studies, we even found that with bacteria-expressed nonglycosylated MHCII, peptide binding was increased over the glycosylated form. Although the mechanism for this increase remains unclear, many biochemical and structural studies on MHC and TCRs have used bacterially expressed protein (Frayser et al., 1999; Li et al., 2000) or baculovirus/insect cell–expressed molecules (Brown et al., 1995; Gauthier et al., 1998) that are characterized by regular, but limited, mannose core structures that lack mammalian complexity and heterogeneity (Altmann et al., 1999). In stark contrast to the wealth of information on conventional peptide antigens, our findings point to a fundamental yet poorly understood difference in the mechanism of interaction between carbohydrate antigens and MHCII in that the native complex N-glycans appear to play a critical functional role during association.

Another function of N-linked glycans is a check on protein folding within the endoplasmic reticulum. The addition of the core $GlcNAc_2Man_9Glc_3$ N-glycan to asparagine residues within the Asn-X-Ser/Thr consensus sequence occurs in the ER. After the initial cleavage of two terminal glucose residues, these structures bind to calnexin and calreticulin, which are thought to be an important check on folding and facilitate MHCII trafficking out of the ER into the Golgi apparatus (Trombetta and Helenius, 1998). However, at least one study reported that treatment of APCs with the N-glycosylation inhibitor tunicamycin failed to alter the plasma membrane concentration of MHCII (Hart, 1982), suggesting that MHCII trafficking to the cell surface is not particularly sensitive to N-linked glycosylation. Indeed, our results support this interpretation in that modification of the N-glycans on MHCII by blocking early steps in the glycosylation pathway did not alter MHCII surface staining or peptide presentation, yet GlyAg presentation was significantly reduced. Unaltered peptide presentation and T cell activation in vitro demonstrate that the MHCII on the cell surface is properly folded and can be normally recognized by cognate TCRs on opposing CD4$^+$ T cells. In vitro binding experiments with MHCII lacking native N-glycans reveal no reduction in peptide binding, but near ablation of GlyAg binding. Confocal microscopy further demonstrates vesicular colocalization of GlyAg and MHCII, confirming that antigen endocytosis and trafficking to the normal MHCII compartment was unaffected by the glycosylation changes. Finally, structural studies using bacterial (Frayser et al., 1999; Li et al., 2000) and insect cell expressed MHCII (Brown et al., 1995; Gauthier et al., 1998) show no significant differences in overall structure. We conclude that although modification of N-glycans directly impacts GlyAg-mediated responses and APC surface localization of GlyAg, this alteration in MHCII antigen presentation activity is not caused by changes in endocytosis, vesicular trafficking, surface

MHCII concentration, or MHCII conformational changes, although we cannot rule out small localized structural variations that do not affect peptide ligands.

It is conceivable that the requirement for large native complex N-glycans on MHCII for GlyAg binding is based on extending the surface area of the binding platform beyond that of the canonical peptide-binding groove. GlyAg and peptide association with MHCII is competitive and GlyAg presentation by APCs is dependent on HLA-DM expression (Cobb and Kasper, 2008; Velez et al., 2009), establishing that bound peptide must be removed before GlyAgs can bind. As a result, GlyAgs likely form contacts within the peptide-binding groove. However, the presented form of GlyAgs ranges in molecular mass between 3 and 10 kD (Cobb et al., 2004; Cobb and Kasper, 2008), which is greater than the typical 13–18-aa peptide found bound to MHCII. Furthermore, we have shown that the helical nature of the GlyAg conformation must be maintained to facilitate MHCII binding (Kreisman et al., 2007). Based on the known structure of MHCII (Gauthier et al., 1998), it is difficult to imagine how the relatively constrained surface area of the peptide-binding groove alone can stably associate with a helical 3–10 kD polysaccharide. Given that complex N-glycans can be the physical size of an immunoglobulin domain (30 Å x 10 Å x 10 Å; Rudd et al., 1999), inclusion of the two conserved sites for MHCII glycosylation could potentially add up to 600 $Å^2$ in surface area on which the GlyAg molecule could associate, although the glycan array results show that these structures alone are insufficient for GlyAg binding. Our findings allow us to speculate that native complex N-glycans, as well as the MHCII protein backbone, form direct contacts with GlyAgs and that modification of these N-glycans destabilizes GlyAg association by removing a physical portion of the binding site.

This study represents the first time that the N-linked glycans on MHCII have been shown to play an integral role in antigen binding. However, in 1995 it was reported that altering the glycosylation sites in $E\alpha^d$ resulted in changes in thymus selection of $V\beta7^+$ T cells (Ishikawa et al., 1995), suggesting that glycosylation can influence the binding of a subset of TCRs, depending on the Vβ usage, although it remains unclear whether this effect was direct (i.e., the glycans participated in the binding) or indirect (e.g., through structural alignment of the binding surfaces). A few years later, the Mellins group reported that creation of a novel glycosylation site at N94 in DRA showed severe defects in peptide antigen presentation (Guerra et al., 1998). It was determined that the new glycan site interfered with HLA-DM–catalyzed ligand exchange on MHCII, and thus had an indirect role in peptide binding.

The nature of glycans expressed by a given cell is dependent on the expression pattern of glycosyltransferases in the Golgi apparatus. It is established, for example, that gastric epithelial cells show varied glycosylation of MHCII as compared with B cells (Barrera et al., 2002). Perhaps more significantly, alterations in cellular protein glycosylation have been reported in inflammatory bowel disease (IBD) and colon cancer patients (Campbell et al., 2001; Bodger et al., 2006). Because the glycosylation pattern seen in human MHCII is known to closely mirror the overall glycosylation pattern found in cell glycoproteins (Néel et al., 1987), this work suggests that MHCII is differentially glycosylated in active IBD and cancer. In strong support of this interpretation, transgenic animals expressing α1,2-fucosyltransferase have significant changes in cellular glycosylation patterns and develop spontaneous colitis (Brown et al., 2004). The etiology of this colitis was found to be centered upon the T cell compartment rather than defects in the mucosal barrier function. Remarkably, the GlyAg used in this study, PSA, has been directly implicated as being a key bacterial factor that contributes to the maintenance of gastric immune balance (Mazmanian et al., 2005, 2008). Specifically, PSA administered to gnotobiotic animals restores the T_H1/T_H2 balance to that of conventionally colonized animals (Mazmanian et al., 2005), and PSA elicits IL-10–producing T cells that show remarkable efficacy in down-regulating inflammation in animal models of IBD (Mazmanian et al., 2008). Because the T cells activated by PSA appear to serve an antiinflammatory/tolerogenic role in the gut, our findings suggest that IBD-associated changes in protein glycosylation (Campbell et al., 2001; Brown et al., 2004) could result in defects in PSA presentation, leading to a failure to induce protective antiinflammatory IL-10–producing T cells and an exacerbation of gut pathology.

MATERIALS AND METHODS

Reagents and cell lines. Human Raji B cells (American Type Culture Collection) were maintained in RPMI 1640 (Invitrogen) media supplemented with 10% FBS, penicillin, streptomycin (pen/strep), and β-mercaptoethanol (βME). CHO cells transfected to secrete soluble human HLA-DR2 (DR2) were provided by K. Wucherpfennig (Dana Farber Cancer Center, Boston, MA; Gauthier et al., 1998) and grown in protein free medium (HyQ SFM-4CHO; HyClone) supplemented without (untreated; UNT) and with 10 μg/ml KF (Cayman Chemical) or 175 μM CS (Sigma-Aldrich). The inhibitors and media were replaced daily. Recombinant DR2 proteins expressed with and without drugs present in the media (UNT-DR2, CS-DR2, and KF-DR2) were purified to homogeneity (>95% purity as judged by SDS-PAGE) from the spent culture media as previously described (Cobb et al., 2004). HEK293 cells expressing murine TLR2 (InvivoGen) were grown in standard DME medium supplemented with 10% FBS. PSA was expressed by a *B. fragilis* variant that expresses only PSA in the capsule (Krinos et al., 2001) and purified to homogeneity, radiolabeled, fluorescently tagged with Alexa Fluor 594, and biotinylated as previously described (Cobb et al., 2004). Biotinylated MBPp (residues 84–99) and OVAp (residues 323–339) were purchased from New England Peptide. mAb specific for HLA-DR (clone L243) was expressed and purified from HB-55 B cell hybridoma supernatants using a recombinant protein A column (GE Healthcare) and labeled with Alexa Fluor 488 according to the manufacturer's protocol (Invitrogen).

Flow cytometry. For in vitro and ex vivo experiments, cells were cultured for 3 d in the presence and absence of 10 μg/ml KF or 175 μM CS. The inhibitors and media were replaced daily. After treatment, the cells were washed in PBS and resuspended in FACS staining buffer (PBS, pH 7.2, 3% FBS, and 0.5% sodium azide) supplemented with either 2 μg Alexa Fluor 488–conjugated L243 mAb or 5 μg FITC-conjugated *Phaseolus vulgaris* leucoagglutinin (PHA-L; Vector Laboratories) for 30 min on ice. Cells were washed twice in PBS before FACS analysis on a C6 flow cytometer (Accuri Cytometers). Staining primary cells from animals was performed using the same protocol. Intracellular cytokine staining was

performed after a 6-h stimulation with 10 ng/ml PMA and 500 nM ionomycin. Analyses of FACS data were performed using FCS Express (De Novo Software).

Confocal microscopy. Raji B cells were incubated in the presence or absence of 10 µg/ml KF or 175 µM CS for 3 d, with fresh drug and media added daily. On the final day, Alexa Fluor 594–conjugated PSA was added to the cells. 24 h later, cells were harvested, washed, and fixed in 4% paraformaldehyde for 30 min on ice. The cells were washed and incubated with Alexa Fluor 488–conjugated L243 mAb for 30 min on ice. The cells were then washed and mounted on coverslips for viewing by confocal microscopy using an SP5 laser scanning confocal microscope (63× oil-immersion objective; Leica). Cross-sectional histograms of the pixel intensities were determined from high-resolution confocal images ($n > 10$ per sample) using the Leica Application Suite software, and then used to calculate the average pixel intensities found within the borders of each cell (vesicular) and those found on the borders of the cells (surface) as described previously (Cobb et al., 2004). Statistical analyses of surface and vesicular-localized signals were performed using an unpaired analysis of variance with Bonferroni Multiple Comparisons post-test with GraphPad InStat software (GraphPad Software).

Antigen processing assays. PSA processing was measured as previously described (Cobb et al., 2004). Raji B cells (10^7) treated with and without 10 µg/ml KF or 175 µM CS for 3 d before antigen exposure were cultured with 0.5 mg [^{3}H]PSA for 15 h at 37°C to allow for endocytosis and processing. Cells were harvested and washed with PBS, and then mechanically lysed by passage through a 27-gauge needle in 250 mM sucrose buffered with 25 mM Tris-HCl, pH 7.5. Microsomes were isolated for analysis of endocytosed glycoantigen by centrifugation at 100,000 *g* for 1 h. The pellet was resuspended in 25 mM Tris, pH 7.5, and 0.5 mg/ml Pronase to eliminate any interactions between PSA and resident proteins for 2 h at 37°C. The resulting sample was then passed through a Superose 12 molecular sieve column fitted to an Äkta Purifier10 HPLC system (GE Healthcare) while collecting fractions. The fractions were analyzed by liquid scintillation counting and graphed by elution volume to determine the molecular size of the glycoantigen fragments isolated from the vesicular compartments of Raji B cells.

Antigen presentation assays. 10^7 Raji B cells untreated or treated with 10 µg/ml KF or 175 µM CS for 3 d before antigen exposure were cultured with 0.25 mg biotin-conjugated PSA or 0.25 mg biotin-conjugated MBPp for 24 h at 37°C to allow for presentation. Cells were harvested, washed, and digested with papain (0.1 mg/ml papain; 10 mM Tris-HCL, pH 7.5; 1 mM EDTA; 1% βME) to release surface-localized MHCII proteins and their interacting antigens (Wiman et al., 1982). Protease inhibitor cocktail (Sigma-Aldrich) was added and the samples incubated in wells of ELISA plates precoated with either 25 µg HLA-DR–specific L243 mAb or IgG2a isotype control overnight at 4°C. The wells were washed and incubated with europium-conjugated streptavidin (Eu-SA; PerkinElmer) for 45 min. The wells were washed again and the biotinylated PSA or MBPp present quantified by time-resolved fluorescence (TRF) on a Victor^{3}V Multilabel Counter using dissociation enhanced fluorescence Enhancement Solution according to the manufacturer's protocol (PerkinElmer). Statistical comparisons between untreated and drug-treated samples with each antigen were performed with a student's *t* test using InStat.

Cell viability assays. 10^5 Raji B cells untreated or treated with 10 µg/ml KF or 175 µM CS for 3 d were cultured in 200 µl of media in wells of a 96-well plate in quadruplicate. At the end of day 3, 50 µl of culture supernatant was removed from each culture well and combined with 50 µl of ATPlite reagent (PerkinElmer) for 5 min. ATP concentration was measured by luminescence on a Victor^{3}V Multilabel Counter as a measure of cell metabolic activity and viability.

Binding assays. The interaction between HLA-DR2 and MBPp or PSA was measured exactly as previously described (Cobb and Kasper, 2008, Kreisman et al., 2007). In brief, 200 ng of each purified recombinant DR2 protein (UNT-DR2, CS-DR2, or KF-DR2) was immobilized in wells of an Immulon 4HBX 384 well ELISA plate. 2.0 µg of either biotinylated, low molecular weight PSA or biotinylated MBPp was incubated in the DR2 or negative control FBS-blocked wells for 24 h at 37°C. For the MBPp binding, the binding was performed in Tris-buffered saline, pH 7.5, while PSA binding was performed in citrate-buffered saline, pH 4.5 as previously reported (Cobb and Kasper, 2008). Bound biotinylated ligand was quantified as described for the coimmunoprecipitation presentation experiments using Eu-SA and TRF on a Victor^{3}V counter. Statistical analyses of the resulting data were performed using a Student's *t* test in InStat.

Lectin ELISA. The nature of N-glycans on CHO-expressed UNT-DR2, CS-DR2, and KF-DR2 proteins was determined by ELISA with several biotinylated lectins (indicated in Fig. 4, D and E; Vector Laboratories). 2 µg of each protein was immobilized in wells of an Immulon 4HBX 96-well ELISA plate and probed with 5 µg/ml of each lectin. Each protein was done in at least triplicate for each of the lectins. Comparisons were made by normalizing the signal to unity for the UNT-DR2 and then calculating the fold change in lectin binding for each of the CS-DR2 and KF-DR2.

Glycan-binding array. High-throughput glycan-binding array screening was performed as described previously (Paulson et al., 2006; von Gunten et al., 2009) by the Core H of the National Institutes of Health–funded Consortium for Functional Glycomics, except Alexa Fluor 488–conjugated PSA was used as the potential glycan binding molecule. The glycan targets immobilized on the array is presented in Table S1.

TLR2 activation. HEK293 cells expressing recombinant TLR2 were grown in 6-well plates in the presence and absence of 10 µg/ml KF or 175 µM CS for 3 d. On day 4, cells were transferred to a 96-well plate at 2×10^4 cells per well. Cells were stimulated for 12 h with either 50 µg/ml PSA, as shown previously (Wang et al., 2006), or 15 nM Pam3Cysk4. Culture supernatants were then analyzed for IL-8 production by sandwich ELISA according to the manufacturer's protocol (BioLegend).

T cell activation (inhibitors). Mouse BM of WT C57BL/6 mice (The Jackson Laboratory) were differentiated into BMDCs by growing them in RPMI 1640 containing 10% FBS, βME, pen/strep, 15 ng/ml GM-CSF (Invitrogen) for 10 d. On days 7–9, BMDCs were treated with 10 µg/ml KF or 175 µM CS. On day 10, BMDCs were collected and verified by flow cytometry using CD11c-specific mAb and cultured for 24 h with and without fresh drugs and antigen (see Results section). On day 11, fresh naive CD4$^+$ T cells were isolated from the spleens of untreated C57BL/6 mice (or OT-II mice for OVAp assays; The Jackson Laboratory) by positive selection using CD4$^+$ magnetic beads (Miltenyi Biotec) and verified by flow cytometry using CD4-specific mAb. CD4$^+$ T cells were then added to the BMDC cultures at a 10:1 ratio (i.e., 10 T cells per BMDC) and the samples were incubated for 3 d (DQ-OVA and OVAp assays) or 4 d (GlyAg assays) without the addition of more CS or KF. Culture supernatants were then analyzed for IFN-γ by sandwich ELISA according to the manufacturer's protocol (BioLegend). Statistical analyses were performed using an unpaired analysis of variance with Bonferroni Multiple Comparisons post-test.

BMDC maturation. As described in the previous section for T cell activation, BMDCs were cultured for 3 d with and without CS and KF. Antigen-induced maturation after 24 h stimulation was measured by cell surface staining and flow cytometry using FITC-conjugated mouse MHCII-specific mAb (clone 25–9-17; BioLegend).

MGat2 experiments. BM cells collected from WT C57BL/6 (MGat2^{wt}) and B6.129-MGat2^{tm1Jxm}/J (MGat2^{flox}) mice (The Jackson Laboratory) were depleted of erythrocytes using Red Blood Cell Lysing Buffer (Sigma-Aldrich). Using the Neon Transfection System and the Neon 100 µl kit (Invitrogen), 5×10^6 cells were electroporated with 6 µg pCAG-Cre (Matsuda and Cepko, 2007)

in 100 µl T-buffer using a single 20 ms, 2,200 V pulse. Transfected BM cells were then cultured with GM-CSF to facilitate BMDC differentiation, as described in the T cell activation (inhibitors) section. The pCAG-Cre plasmid was supplied by C. Cepko (Harvard University, Boston, MA) through the Addgene depository (Addgene plasmid 13775). Cells expressing CRE were selected and purified based on PHA-L staining. In brief, MGat2^{flox} BMDCs previously transfected with pCAG-Cre were labeled with 20 µg/ml biotinylated PHA-L (Vector Laboratories) and anti-biotin magnetic microbeads then passed through a magnetic MACS LS column (Miltenyi Biotec). The non-binding cells (PHA-L negative) found in the flow through (MGat2^{neg}) were analyzed by RT-PCR (see the RT-PCR section), and flow cytometry for purity using biotin-PHA-L and a fluorescent streptavidin-APC conjugate (BioLegend) and compared with MGat2^{wt} cells (MGat2^{pos}). For T cell assays using MGat2^{pos} and MGat2^{neg} BMDCs, CD4$^+$ T cells were isolated from the spleens of C57BL/6 or OT-II mice (The Jackson Laboratory) by positive selection using CD4$^+$ magnetic beads (Miltenyi Biotec). CD4$^+$ T cells were added to the BMDC cultures at a 10:1 ratio (i.e., 10 T cells per BMDC) in the presence or absence of 50 µg/ml OVA or PSA. Activation was assessed on day 3 using IFN-γ production by sandwich ELISA according to the manufacturer's protocol (BioLegend).

Western blots. Protein extracts were prepared from BM cells 18 h after transfection with the CRE recombinase expression construct pCAG-Cre (see above). In brief, cells were lysed for 30 min in 20 mM Tris-HCl, pH 7.5, 150 mM NaCl, 1% NP-40, and Complete Mini protease inhibitor cocktail (Roche). Protein samples were normalized using the microBCA Protein Assay kit (Thermo Fisher Scientific) before separation by SDS-PAGE and transfer to an Immobilon-P membrane (Millipore). Membranes were probed with either rabbit anti-CRE (Immuno-Biological Laboratories), rabbit anti-myc (Cell Signaling Technology), or mouse anti–β-actin (clone 2F1-1; BioLegend) antibodies, followed by HRP-conjugated secondary antibodies. Visualization was performed on film using ECL Plus (GE Healthcare) or ECL (Thermo Fisher Scientific).

***MGat2* RT-PCR.** RNA was isolated from both BMDC populations using the PerfectPure RNA Cell and Tissue kit (5 Prime) to verify the presence or absence of *MGat2* transcription. Using equal amounts of RNA, mRNA reverse transcription and PCR were performed using the SuperScript III First-Strand Synthesis System for RT-PCR kit following the manufacturer's instructions (Invitrogen). Primers used for PCR (IDT) were as follows: *MGat2*, forward 5′-TTGCTGATAGACTCGCTTCG-3′ and reverse 5′-GCTGAACGGAAAGAACACTTG-3′; β-actin, forward 5′-TGAGAGGGAAATCGTGCGTGA-3′ and reverse 5′-CACTATTGGCAACGAGCGGTTC-3′.

Animal studies. C57BL/6 mice were bred and maintained in a specific pathogen–free environment at Case Western Reserve University and were treated under IACUC-approved guidelines in accordance with approved protocols. All injections were given i.p. Age-matched C57BL/6 mice were treated with 250 µg KF (dissolved in PBS at 1 mg/ml) or PBS alone for three consecutive days. Where indicated, some mice received a cell transfer (i.p.) of 5×10^6 WT APCs on day 4, 2 h before additional treatments. On day 4, all mice received an additional dose of KF or PBS, including a sensitizing dose consisting of 100 µg purified PSA or 100 µg OVA protein (Sigma-Aldrich) with a 1:3-1:5 dilution of sterilized cecal contents (Cobb et al., 2004) in a final volume of 200 µl PBS. At the indicated time point after immunization, spleens were harvested to assay antigen-specific CD4$^+$ T cell recall responses. In brief, CD4$^+$ T cells were purified by positive selection using CD4 magnetic labeling beads per the manufacturer instructions (Miltenyi Biotec). APCs were isolated from splenocyte populations after depletion of T cells using CD90.2 magnetic labeling beads per the manufacturer's instructions (Miltenyi Biotec). 2.5×10^5 CD4$^+$ T cells and 2.5×10^5 APCs were added per well in triplicate with or without 50 µg/ml antigen in a final volume of 200 µl RPMI 1640 media (Invitrogen) supplemented with 10% FBS, pen/strep, L-glutamine, and βME. Supernatants were assayed for the presence of IFN-γ by ELISA according to the manufacturer's protocol (eBioscience). Statistical analyses of the resulting data were performed using an unpaired Student's *t* test.

Online supplemental material. Table S1 shows the Consortium for Functional Glycomics Glycan Array Information List of all glycans represented on the glycan-binding array. Fig. S1 shows BMDC control analyses. Online supplemental material is available at http://www.jem.org/cgi/content/full/jem.20100508/DC1.

The authors wish to thank Colleen Lewis, Lili Zhang, and Luke Bury for technical assistance. We also thank Lori Kreisman for critical evaluation of this manuscript, Richard Cummings for helpful discussions and experimental advice, and Derek Abbott for technical advice, Western blot antibodies, and the use of his Neon transfection system instrument. We thank Dr. Roy Marriuza for supplying *Escherichia coli*–expressed HLA-DR protein.

The glycan-binding array was performed by Core H of the Consortium for Functional Glycomics, which is funded by grant GM062116 through the National Institute of General Medical Sciences. This work was funded by grants OD004225 and GM082916 to B.A. Cobb.

The authors claim no competing financial interests.

Submitted: 12 March 2010
Accepted: 17 March 2011

REFERENCES

Altmann, F., E. Staudacher, I.B. Wilson, and L. März. 1999. Insect cells as hosts for the expression of recombinant glycoproteins. *Glycoconj. J.* 16:109–123. doi:10.1023/A:1026488408951

Barrera, C., R. Espejo, and V.E. Reyes. 2002. Differential glycosylation of MHC class II molecules on gastric epithelial cells: implications in local immune responses. *Hum. Immunol.* 63:384–393.

Bergeron, J.J., A. Zapun, W.J. Ou, R. Hemming, F. Parlati, P.H. Cameron, and D.Y. Thomas. 1998. The role of the lectin calnexin in conformation independent binding to N-linked glycoproteins and quality control. *Adv. Exp. Med. Biol.* 435:105–116.

Bodger, K., J. Halfvarson, A.R. Dodson, F. Campbell, S. Wilson, R. Lee, E. Lindberg, G. Järnerot, C. Tysk, and J.M. Rhodes. 2006. Altered colonic glycoprotein expression in unaffected monozygotic twins of inflammatory bowel disease patients. *Gut.* 55:973–977. doi:10.1136/gut.2005.086413

Brown, J.H., T.S. Jardetzky, L.J. Stern, J.C. Gorga, J.L. Strominger, and D.C. Wiley. 1995. Human class II MHC molecule HLA-DR1: X-ray structure determined from three crystal forms. *Acta Crystallogr. D Biol. Crystallogr.* 51:946–961. doi:10.1107/S0907444995002289

Brown, S.J., A.M. Miller, P.J. Cowan, J. Slavin, W.R. Connell, G.T. Moore, S. Bell, P.R. Elliott, P.V. Desmond, and A.J. d'Apice. 2004. Altered immune system glycosylation causes colitis in alpha1,2-fucosyltransferase transgenic mice. *Inflamm. Bowel Dis.* 10:546–556. doi:10.1097/00054725-200409000-00008

Brubaker, J.O., Q. Li, A.O. Tzianabos, D.L. Kasper, and R.W. Finberg. 1999. Mitogenic activity of purified capsular polysaccharide A from *Bacteroides fragilis*: differential stimulatory effect on mouse and rat lymphocytes in vitro. *J. Immunol.* 162:2235–2242.

Campbell, B.J., L.G. Yu, and J.M. Rhodes. 2001. Altered glycosylation in inflammatory bowel disease: a possible role in cancer development. *Glycoconj. J.* 18:851–858. doi:10.1023/A:1022240107040

Choi, Y.H., M.H. Roehrl, D.L. Kasper, and J.Y. Wang. 2002. A unique structural pattern shared by T-cell-activating and abscess-regulating zwitterionic polysaccharides. *Biochemistry.* 41:15144–15151. doi:10.1021/bi020491v

Cobb, B.A., and D.L. Kasper. 2008. Characteristics of carbohydrate antigen binding to the presentation protein HLA-DR. *Glycobiology.* 18:707–718. doi:10.1093/glycob/cwn050

Cobb, B.A., Q. Wang, A.O. Tzianabos, and D.L. Kasper. 2004. Polysaccharide processing and presentation by the MHCII pathway. *Cell.* 117:677–687. doi:10.1016/j.cell.2004.05.001

Dustin, M.L., L.M. Ferguson, P.Y. Chan, T.A. Springer, and D.E. Golan. 1996. Visualization of CD2 interaction with LFA-3 and determination of the two-dimensional dissociation constant for adhesion receptors in a contact area. *J. Cell Biol.* 132:465–474. doi:10.1083/jcb.132.3.465

Dustin, M.L., D.E. Golan, D.M. Zhu, J.M. Miller, W. Meier, E.A. Davies, and P.A. van der Merwe. 1997. Low affinity interaction of human or rat T cell adhesion molecule CD2 with its ligand aligns adhering membranes

to achieve high physiological affinity. *J. Biol. Chem.* 272:30889–30898. doi:10.1074/jbc.272.49.30889

Frayser, M., A.K. Sato, L. Xu, and L.J. Stern. 1999. Empty and peptide-loaded class II major histocompatibility complex proteins produced by expression in *Escherichia coli* and folding in vitro. *Protein Expr. Purif.* 15:105–114. doi:10.1006/prep.1998.0987

Gauthier, L., K.J. Smith, J. Pyrdol, A. Kalandadze, J.L. Strominger, D.C. Wiley, and K.W. Wucherpfennig. 1998. Expression and crystallization of the complex of HLA-DR2 (DRA, DRB1*1501) and an immunodominant peptide of human myelin basic protein. *Proc. Natl. Acad. Sci. USA.* 95:11828–11833. doi:10.1073/pnas.95.20.11828

Guerra, C.B., R. Busch, R.C. Doebele, W. Liu, T. Sawada, W.W. Kwok, M.D. Chang, and E.D. Mellins. 1998. Novel glycosylation of HLA-DRalpha disrupts antigen presentation without altering endosomal localization. *J. Immunol.* 160:4289–4297.

Hart, G.W. 1982. The role of asparagine-linked oligosaccharides in cellular recognition by thymic lymphocytes. Effects of tunicamycin on the mixed lymphocyte reaction. *J. Biol. Chem.* 257:151–158.

Ishikawa, S., C. Kowal, B. Cole, C. Thomson, and B. Diamond. 1995. Replacement of N-glycosylation sites on the MHC class II E alpha chain. Effect on thymic selection and peripheral T cell activation. *J. Immunol.* 154: 5023–5029.

Kreisman, L.S., J.H. Friedman, A. Neaga, and B.A. Cobb. 2007. Structure and function relations with a T-cell-activating polysaccharide antigen using circular dichroism. *Glycobiology.* 17:46–55. doi:10.1093/glycob/cwl056

Krinos, C.M., M.J. Coyne, K.G. Weinacht, A.O. Tzianabos, D.L. Kasper, and L.E. Comstock. 2001. Extensive surface diversity of a commensal microorganism by multiple DNA inversions. *Nature.* 414:555–558. doi:10.1038/35107092

Lewis, C.J., and B.A. Cobb. 2010. Carbohydrate oxidation acidifies endosomes, regulating antigen processing and TLR9 signaling. *J. Immunol.* 184:3789–3800. doi:10.4049/jimmunol.0903168

Li, Y., H. Li, R. Martin, and R.A. Mariuzza. 2000. Structural basis for the binding of an immunodominant peptide from myelin basic protein in different registers by two HLA-DR2 proteins. *J. Mol. Biol.* 304:177–188. doi:10.1006/jmbi.2000.4198

Li, Y., H. Li, N. Dimasi, J.K. McCormick, R. Martin, P. Schuck, P.M. Schlievert, and R.A. Mariuzza. 2001. Crystal structure of a superantigen bound to the high-affinity, zinc-dependent site on MHC class II. *Immunity.* 14:93–104. doi:10.1016/S1074-7613(01)00092-9

Matsuda, T., and C.L. Cepko. 2007. Controlled expression of transgenes introduced by in vivo electroporation. *Proc. Natl. Acad. Sci. USA.* 104:1027–1032. doi:10.1073/pnas.0610155104

Mazmanian, S.K., C.H. Liu, A.O. Tzianabos, and D.L. Kasper. 2005. An immunomodulatory molecule of symbiotic bacteria directs maturation of the host immune system. *Cell.* 122:107–118. doi:10.1016/j.cell.2005.05.007

Mazmanian, S.K., J.L. Round, and D.L. Kasper. 2008. A microbial symbiosis factor prevents intestinal inflammatory disease. *Nature.* 453:620–625. doi:10.1038/nature07008

Néel, D., B. Merlu, E. Turpin, C. Rabourdin-Combe, B. Mach, Y. Goussault, and D.J. Charron. 1987. Characterization of N-linked oligosaccharides of an HLA-DR molecule expressed in different cell lines. *Biochem. J.* 244:433–442.

Paulson, J.C., O. Blixt, and B.E. Collins. 2006. Sweet spots in functional glycomics. *Nat. Chem. Biol.* 2:238–248. doi:10.1038/nchembio785

Rudd, P.M., M.R. Wormald, R.L. Stanfield, M. Huang, N. Mattsson, J.A. Speir, J.A. DiGennaro, J.S. Fetrow, R.A. Dwek, and I.A. Wilson. 1999. Roles for glycosylation of cell surface receptors involved in cellular immune recognition. *J. Mol. Biol.* 293:351–366. doi:10.1006/jmbi.1999.3104

Rudd, P.M., T. Elliott, P. Cresswell, I.A. Wilson, and R.A. Dwek. 2001. Glycosylation and the immune system. *Science.* 291:2370–2376. doi:10.1126/science.291.5512.2370

Saito, Y., Y. Ihara, M.R. Leach, M.F. Cohen-Doyle, and D.B. Williams. 1999. Calreticulin functions in vitro as a molecular chaperone for both glycosylated and non-glycosylated proteins. *EMBO J.* 18:6718–6729. doi:10.1093/emboj/18.23.6718

Stephen, T.L., M. Niemeyer, A.O. Tzianabos, M. Kroenke, D.L. Kasper, and W.M. Kalka-Moll. 2005. Effect of B7-2 and CD40 signals from activated antigen-presenting cells on the ability of zwitterionic polysaccharides to induce T-Cell stimulation. *Infect. Immun.* 73:2184–2189. doi:10.1128/IAI.73.4.2184-2189.2005

Stingele, F., B. Corthésy, N. Kusy, S.A. Porcelli, D.L. Kasper, and A.O. Tzianabos. 2004. Zwitterionic polysaccharides stimulate T cells with no preferential V beta usage and promote anergy, resulting in protection against experimental abscess formation. *J. Immunol.* 172:1483–1490.

Trombetta, E.S., and A. Helenius. 1998. Lectins as chaperones in glycoprotein folding. *Curr. Opin. Struct. Biol.* 8:587–592. doi:10.1016/S0959-440X(98)80148-6

Tzianabos, A.O., A. Pantosti, H. Baumann, J.R. Brisson, H.J. Jennings, and D.L. Kasper. 1992. The capsular polysaccharide of *Bacteroides fragilis* comprises two ionically linked polysaccharides. *J. Biol. Chem.* 267: 18230–18235.

Tzianabos, A.O., A.B. Onderdonk, B. Rosner, R.L. Cisneros, and D.L. Kasper. 1993. Structural features of polysaccharides that induce intra-abdominal abscesses. *Science.* 262:416–419. doi:10.1126/science.8211161

Tzianabos, A.O., D.L. Kasper, and A.B. Onderdonk. 1995. Structure and function of *Bacteroides fragilis* capsular polysaccharides: relationship to induction and prevention of abscesses. *Clin. Infect. Dis.* 20:S132–S140. doi:10.1093/clinids/20.Supplement_2.S132

Tzianabos, A.O., J.Y. Wang, and J.C. Lee. 2001. Structural rationale for the modulation of abscess formation by Staphylococcus aureus capsular polysaccharides. *Proc. Natl. Acad. Sci. USA.* 98:9365–9370. doi:10.1073/pnas.161175598

Velez, C.D., C.J. Lewis, D.L. Kasper, and B.A. Cobb. 2009. Type I Streptococcus pneumoniae carbohydrate utilizes a nitric oxide and MHC II-dependent pathway for antigen presentation. *Immunology.* 127:73–82. doi:10.1111/j.1365-2567.2008.02924.x

von Gunten, S., D.F. Smith, R.D. Cummings, S. Riedel, S. Miescher, A. Schaub, R.G. Hamilton, and B.S. Bochner. 2009. Intravenous immunoglobulin contains a broad repertoire of anticarbohydrate antibodies that is not restricted to the IgG2 subclass. *J. Allergy Clin. Immunol.* 123:1268–1276: e15. doi:10.1016/j.jaci.2009.03.013

Wang, Y., W.M. Kalka-Moll, M.H. Roehrl, and D.L. Kasper. 2000. Structural basis of the abscess-modulating polysaccharide A2 from *Bacteroides fragilis*. *Proc. Natl. Acad. Sci. USA.* 97:13478–13483. doi:10.1073/pnas.97.25.13478

Wang, Y., J. Tan, M. Sutton-Smith, D. Ditto, M. Panico, R.M. Campbell, N.M. Varki, J.M. Long, J. Jaeken, S.R. Levinson, et al. 2001. Modeling human congenital disorder of glycosylation type IIa in the mouse: conservation of asparagine-linked glycan-dependent functions in mammalian physiology and insights into disease pathogenesis. *Glycobiology.* 11:1051–1070. doi:10.1093/glycob/11.12.1051

Wang, Q., R.M. McLoughlin, B.A. Cobb, M. Charrel-Dennis, K.J. Zaleski, D. Golenbock, A.O. Tzianabos, and D.L. Kasper. 2006. A bacterial carbohydrate links innate and adaptive responses through Toll-like receptor 2. *J. Exp. Med.* 203:2853–2863. doi:10.1084/jem.20062008

Wiman, K., L. Claesson, L. Rask, L. Trägårdh, and P.A. Peterson. 1982. Purification and partial amino acid sequence of papain-solubilized class II transplantation antigens. *Biochemistry.* 21:5351–5358. doi:10.1021/bi00264a036

Wormald, M.R., and R.A. Dwek. 1999. Glycoproteins: glycan presentation and protein-fold stability. *Structure.* 7:R155–R160. doi:10.1016/S0969-2126(99)80095-1